

Beyond Periodicity: Towards a Unifying Framework for Activations in Coordinate-MLPs

Sameera Ramasinghe*

Simon Lucey

Australian Institute for Machine Learning
University of Adelaide

Abstract

Coordinate-MLPs are emerging as an effective tool for modeling multidimensional continuous signals, overcoming many drawbacks associated with discrete grid-based approximations. However, coordinate-MLPs with ReLU activations, in their rudimentary form, demonstrate poor performance in representing signals with high fidelity, promoting the need for positional embedding layers. Recently, Sitzmann et al. [39] proposed a sinusoidal activation function that has the capacity to omit positional embedding from coordinate-MLPs while still preserving high signal fidelity. Despite its potential, ReLUs are still dominating the space of coordinate-MLPs; we speculate that this is due to the hyper-sensitivity of networks – that employ such sinusoidal activations – to the initialization schemes. In this paper, we attempt to broaden the current understanding of the effect of activations in coordinate-MLPs, and show that there exists a broader class of activations that are suitable for encoding signals. We affirm that sinusoidal activations are only a single example in this class, and propose several **non-periodic** functions that empirically demonstrate more robust performance against random initializations than sinusoids. Finally, we advocate for a shift towards coordinate-MLPs that employ these non-traditional activation functions due to their high performance and simplicity.

1. Introduction

Despite the ubiquitous and successful usage of conventional discrete representations in machine learning (e.g. images, 3D meshes, and 3D point clouds etc.), coordinate MLPs are now emerging as a unique instrument that can represent multidimensional signals as continuously differentiable entities. Coordinate-MLPs – also known as *implicit neural representations* [39] – are fully connected networks that encode continuous signals as weights, consuming low-dimensional coordinates as inputs. Such continu-

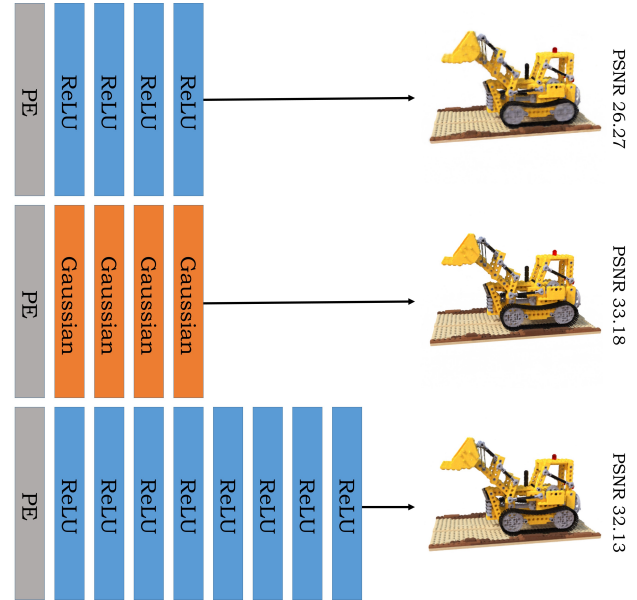


Figure 1. **ReLU vs Gaussian activations (ours)**. Gaussian activations achieve better results with $\sim 50\%$ less parameters. These non-periodic activations are robust to different random initializations of coordinate-MLPs than the sinusoid activations advocated in SIREN [39]

ous representations are powerful compared to their discrete grid-based counterparts, as they can be queried up to extremely high resolutions. Furthermore, whereas the memory consumption of grid-based representations entails exponential growth rates against the dimension and the resolution of data, neural representations have displayed a much more compact relationship between the above factors. Consequently, this recent trend has influenced a proliferation of studies in vision-related research including texture generation [11, 11, 26, 47], shape representation [1, 5, 7, 10, 23, 27, 43], and novel view synthesis [21, 22, 25, 28, 30, 30, 33, 34, 40, 44, 48].

Notwithstanding the virtues mentioned above, coordinate MLPs, in their fundamental form, exhibit poor perfor-

*sameera.ramasinghe@adelaide.edu.au

mance in encoding signals with high-frequency components when equipped with common activation functions such as ReLUs. An elemental reason behind this has shown to be the *spectral bias* of MLPs [2,31]. That is, the corresponding neural tangent kernel (NTK) of MLPs are prone to high-frequency fall-offs, hampering their ability to learn high-frequency functions. The prevalent work-around to this problem involves applying a *positional embedding layer* prior to the MLP, where the low-dimensional inputs are projected to a higher-dimensional space using Fourier features [42].

In contrast, Sitzmann *et al.* [39] recently portrayed that MLPs with sinusoidal activation functions are naturally suited for encoding high-frequency signals, eliminating the need for positional embedding layers. Despite its potential, much of the research that involve coordinate-MLPs still prefer positional embeddings over sinusoidal activations. We postulate that this could be for two reasons. First, Sitzmann *et al.* mainly attributed the success of sinusoidal activations to their periodicity, although the evidence for this relationship still remains scant. Consequently, this lack of understanding obfuscates some of the fundamental principles behind its effectiveness and hampers faithful usage in a wider range of applications. Second, sinusoidal activations are highly sensitive to the initialization of the MLP, showcasing drastic performance drops in cases where the MLP is initialized without strictly adhering to the guidelines of Sitzmann *et al.* The above drawbacks have heightened the need for a more rigorous analysis that facilitates more effective usage of activation functions in coordinate-MLPs.

Contributions: We offer a broader theoretical understanding of the role of activation functions within coordinate-MLPs. In particular, we show that the efficacy of a coordinate-MLP is critically bound to its Lipschitz smoothness and the eigenvalue distribution of the hidden-layer representations, and the optimal values of these metrics depend on the characteristics of the signal that needs to be encoded. We further show that the above properties are inherently linked to each other, and by controlling one property, the other can be implicitly manipulated. We further derive formulae to connect the Lipschitz smoothness and the eigenvalue distribution to the properties of the activation functions. The significance of this finding is two-fold: (i) providing guidelines for tuning the hyper-parameters of an activation function based on the given signal and, (ii) enabling a practitioner to theoretically predict the effect of a given activation function when used in a coordinate-MLP, prior to practical implementation. We further show that sinusoidal activations are simply a single example that fulfills such constraints, and the periodicity is not a crucial factor that determine the efficacy of an activation function. Consequently, we propose a much broader class of *non-periodic* activation functions that can be used in encoding

functions/signals with high fidelity, and show that their empirical properties match with theoretical predictions. We further illustrate that the newly proposed activation functions are robust to different initialization schemes, unlike sinusoidal activations. Further, picking one such proposed activation – Gaussian – as an example, we demonstrate that coordinate-MLPs with such activation functions enjoy better results, faster convergence rates, and shallower architectures in comparison to ReLU-MLPs. Finally, we show that these activations allow positional-embedding-free architectures to be used in complex tasks such as 3D view synthesis. To our knowledge, this is the first instance coordinate-MLPs have successfully been employed in such experiments in the absence of positional embeddings.

2. Related works

Activation functions: (Non-linear) activation functions are an essential component of *any* model that aims to model the relationship between complex functions and their coordinates. These activations significantly broaden the class of signals/functions one can approximate. The role of activation functions have been studied extensively since the earliest days of neural network research [3, 8, 24, 45]. Perhaps, the first notable discussion about the theoretical properties of activations was presented by Williams *et al.* [45], where invariance of non-linearities under logical and ordinal preserving transformation of inputs was explored. Dasgupta *et al.* [6] compared the approximation power of feedforward neural nets with different activations. This initial work was followed by a series of analytical studies including discontinuous [12, 13, 19], polynomial-based [20] and Lipschitz bounded [4, 16, 17] activation functions. In addition to this, a plethora of empirical research has also been published [14, 29, 32, 36, 37]. Periodic non-linearities have also been explored in terms of Fourier feature networks [9, 38], recurrent neural networks [15, 18], and classification tasks [41, 46].

Coordinate MLPs: In recent years, there has been an increasing interest in parameterizing signals using neural networks (also known as coordinate-MLPs), largely owing to the seminal work by Mildenhall *et al.* [22]. The usage of coordinate-MLPs are somewhat different from conventional MLPs: i) conventional MLPs typically operate on high dimensional inputs such as images, sounds, or 3D shapes, and ii) are primarily being used for classification purposes where the decision boundaries do not have to preserve smoothness. In contrast, coordinate-MLPs are used to encode the signals as weights where the inputs are low-dimensional coordinates and the outputs have to preserve smoothness [49]. One of the most remarkable aspects of Mildenhall *et al.*'s work includes demonstrating the generalization properties of such neural signal representations, *i.e.* once trained with a handful of

view points, the coordinate-MLP can reconstruct the view projection from an arbitrary angle with fine-details. This ground-breaking demonstration caused a ripple of studies that include neural signal representations as the core entities across many applications including shape representation [1, 5, 7, 10, 23, 27, 43], and novel view synthesis [21, 22, 25, 28, 30, 30, 33, 34, 40, 44, 48]. However, for optimal performance, these coordinate-MLPs have to use positional embeddings, which allow them to encode high-frequency functions. In contrast, Sitzmann *et al.* [39] proposed sinusoid activations that enables coordinate-MLPs to encode signals with higher quality without positional embeddings. However, sinusoid activations have shown to be extremely sensitive to the initialization scheme of the MLPs. Also, the framework developed by Sitzmann *et al.* is confined to periodic activations. In contrast, our work generalizes the current understanding on the effect of activations in coordinate-MLPs and thereby propose a class of non-periodic activations that is robust under random initializations.

3. Methodology

Notation. The set of real n -dimensional vectors are denoted by \mathbb{R}^n . The vectors are denoted by bold lower-case letters (e.g., \mathbf{x}). The set of $m \times n$ dimensional matrices are denoted by $\mathbb{R}^{m \times n}$, and the matrices are denoted by bold upper-case letters (e.g., \mathbf{A}). \mathbb{S}_r^n and \mathbb{B}_r^n represent the surface of the n -dimensional hyper-sphere and the n -dimensional ball, with radius r . $\|\cdot\|$ denotes vector norm, $\|\cdot\|_F$ denotes the Frobenius norm, and $\|\cdot\|_o$ is the operator norm. $\mathbf{J}(f)_{\mathbf{x}}$ is the Jacobian of f evaluated at \mathbf{x} and $\mathbf{A} \cdot \mathbf{x}$ denotes the matrix multiplication between \mathbf{A} and \mathbf{x} .

Outline: This section is organized as follows. In Section 3.1, we focus on the ability of an MLP to *memorize* data and establish its connection to the rank of the hidden-layer representations. Section 3.2 explores the generalization of an MLP and connects it to the smoothness of the hidden-layer representation. In Section 3.3, we show that the above factors are naturally tied to each other and face an implicit trade-off. Finally, Section 3.4 connects the developed insights from the previous sections to the properties of activation functions.

3.1. Rank and memorization

The efficacy of a coordinate-MLP largely depends on its ability to memorize training data. The objective of this section is to identify the key factors that affect memorization. To establish the foundation for our analysis, we first revisit the formulation of an MLP.

An MLP with $k-1$ non linear hidden-layers with a linear layer at the top can be described by the following equation:

$$\mathbf{y} = g^k \circ \psi^{k-1} \circ g^{k-1} \circ \dots \circ \psi^1 \circ g^1(\mathbf{x}^0), \quad (1)$$

where $g^i : \mathbf{x} \rightarrow \mathbf{A}^i \cdot \mathbf{x} + \mathbf{b}^i$ is an affine projection with trainable weights $\mathbf{A}^i \in \mathbb{R}^{\dim(\mathbf{x}^i) \times \dim(\mathbf{x}^{i-1})}$, $\mathbf{b}^i \in \mathbb{R}^{\dim(\mathbf{x}^i)}$ is the bias, and ψ^i is a non-linear function. Then, the final layer is essentially a linear classifier, acting on a D -dimensional non-linear embedding $\phi(\mathbf{x}^0)$ that projects the low-dimensional coordinates \mathbf{x}^0 to a subspace in \mathbb{R}^D , where $\dim(\mathbf{x}^{k-1}) = D$. If the number of training points is N , we define the total (training) embedding matrix as

$$\mathbf{X} \in \mathbb{R}^{D \times N} := [\phi(\mathbf{x}_1^0)^T \phi(\mathbf{x}_2^0)^T \dots \phi(\mathbf{x}_N^0)^T]^T. \quad (2)$$

Recall that the final layer of an MLP is (typically) an affine projection without any non-linearity. Dropping the bias for simplified notation, we get,

$$\mathbf{Y} = \mathbf{A}^k \cdot \mathbf{X}, \quad (3)$$

where $\mathbf{Y} \in \mathbb{R}^{q \times N}$ and q is the dimension of the outputs. Observe that each row of \mathbf{Y} is a linear combination of the rows of \mathbf{X} . Assume we have no prior knowledge of \mathbf{Y} , that is, the rows of \mathbf{Y} can be *any* arbitrary vector in \mathbb{R}^N . On the other hand, if the rows of \mathbf{X} are linearly independent, they form a basis for \mathbb{R}^N . Therefore, if $\text{rank}(\mathbf{X}) = N$, it is guaranteed that (assuming perfect convergence) the MLP can find a weight matrix \mathbf{A}^k that ensures perfect reconstruction of \mathbf{Y} . Rigorously speaking, the analysis so far only considered the penultimate layer. However, based on the gathered insights, we make the following general claim: *the potential of the hidden-layers to induce representations with higher-ranks correlates with the memorization capacity of a coordinate-MLP. Equivalently, the eigenvalues of the representation should be non-zero.*

However, a critical component is overlooked in the above analysis. In many applications that utilize coordinate-MLPs, the ability predict values at unseen test coordinates is an important attribute. For instance, in novel view synthesis of a 3D scene, the network only observes a handful of views, in which the network then has to predict the views from new angles. Therefore, the immediate question arises *is having non-zero eigenvalues enough?* In Section 3.2, we shall see that this is indeed not the case.

3.2. Smoothness and generalization

In this section, we show that the generalization of a coordinate-MLP is tightly linked to the *local smoothness* of the representation with respect to the variations of the output.

Proposition 1 *Let $f(x) : \mathbb{R} \rightarrow \mathbb{R}$ and $\mathbf{y} = [y_1, y_2, \dots, y_n]$, $\mathbf{x} = [x_1, x_2, \dots, x_n]$ be sampled targets and inputs from f , respectively. Let $\phi(x_i) : \mathbb{R} \rightarrow \mathbb{R}^D$ be a D -dimensional embedding. Say we train a linear classifier and obtain $\mathbf{A} \in \mathbb{R}^{1 \times D}$ such that $y_i = \mathbf{A} \phi(x_i)$, $\forall y_i \in$*

$\mathbf{y}, x_i \in \mathbf{x}$. In order to guarantee the regression of a pair of unseen points (\bar{y}, \bar{x}) as $\bar{y} = \mathbf{A}\phi(\bar{x})$ where $\bar{y} = f(\bar{x})$ and $x_j < \bar{x} < x_i$, the smoothness constraint $\|\phi(x_i) - \phi(x_j)\| = K|x_i - x_j|$ should hold locally. Here, x_i, x_j belong to an open interval around \bar{x} . It follows that as $|x_i - x_j| \rightarrow 0$, $K \propto \frac{d(f(x))}{dx}$ for $x_j < x < x_i$.

Although the above condition seems overly restrictive, recall that the embeddings $\phi(\cdot)$ are learned via hidden-layers, as opposed to being analytically designed. Therefore, it is enough to reduce the search space of the parameters accordingly, as opposed to explicitly enforcing the above constraint. Thus, we can slightly relax the above equality to an inequality in terms of the Lipschitz smoothness. More precisely, in practice, it is enough to ensure

$$\|\phi(\mathbf{x}_1^0) - \phi(\mathbf{x}_2^0)\| \leq C\|\mathbf{x}_1^0 - \mathbf{x}_2^0\|, \quad (4)$$

locally, where the non-negative constant C depends on the magnitude of the local first-order derivatives (*i.e.*, frequencies) of the encoded signal (because C is a surrogate for K in Proposition 1). That is, when encoding a high-frequency signal, C needs to be higher, and vice-versa. From this point on wards, we drop the superscript from \mathbf{x}_i^0 to avoid cluttered notation.

Thus far, we have established that the eigenvalues of the \mathbf{X} correlates with the memorization of seen coordinates and the smoothness of $\phi(\cdot)$ correlates with the generalization performance of an MLP. Thus, it is intriguing to investigate if there exists a connection between these two forces at a fundamental level, as such an analysis has the potential to provide valuable insights that enables efficient manipulation of these factors.

3.3. Smoothness vs. eigenvalue distribution

This section is devoted to exploring the interrelation between the smoothness and the eigenvalue distribution of the hidden representations.

For simplicity, assume that for coordinates \mathbf{x}_i in a given small neighborhood, the corresponding $\{\phi(\mathbf{x}_i)\}_{i=1}^N$ lies on \mathbb{S}_r^D . Further assume that $\phi(\cdot)$ is Lipschitz bounded with a constant C . Then,

$$(\phi(\mathbf{x}_1)\phi(\mathbf{x}_1)^T - 2\phi(\mathbf{x}_1)\phi(\mathbf{x}_2)^T + \phi(\mathbf{x}_2)\phi(\mathbf{x}_2)^T) \leq C\|\mathbf{x}_1 - \mathbf{x}_2\| \quad (5)$$

$$2 \frac{(r^2 - \phi(\mathbf{x}_1)\phi(\mathbf{x}_2)^T)}{\|\mathbf{x}_1 - \mathbf{x}_2\|} \leq C \quad (6)$$

With Eq. 6 in hand, let us consider two cases for \mathbf{X} .

Case 1 *The rows of \mathbf{X} are orthogonal.*

In this case, the rows of \mathbf{X} are mutually perpendicular and the eigenvalues $\{\lambda_i\}_{i=1}^N$ of $\mathbf{X}^T\mathbf{X}$ are identically distributed. Also, one can see that,

$$\lim_{\|\mathbf{x}_1 - \mathbf{x}_2\| \rightarrow 0} C = \infty. \quad (7)$$

In other words, having (approximately) equally distributed eigenvalues violates the Lipschitz smoothness of the network.

Case 2 *The rows of \mathbf{X} are linearly independent and the angle between the rows are upper-bounded by $0 < \alpha < \frac{\pi}{2}$.*

In this case,

$$2 \frac{(r^2 - \phi(\mathbf{x}_1)\phi(\mathbf{x}_2)^T)}{\|\mathbf{x}_1 - \mathbf{x}_2\|} \leq 2r^2 \frac{(1 - \cos(\alpha))}{\|\mathbf{x}_1 - \mathbf{x}_2\|} \leq C. \quad (8)$$

Note that if α is extremely small, it can result in extremely small Lipschitz constants, which can obstruct encoding functions with high frequency components. Moreover, in this scenario, the total energy of the eigenvalues are mainly concentrated on the first few components. As α gets larger, the Lipschitz constant becomes larger, allowing the freedom to equally disperse the energy between eigenvalues. However, note that rigorously speaking, having a larger Lipschitz constant does not automatically ensure having a high energy distribution between the Eigenvalues, since the right-hand side of Eq. 6 is only an upper-bound. Nevertheless, we observed that, in practice, a monotonic relationship between α and C almost always holds. This analysis provides an important intuition: The Lipschitz constant C of the function induced by the hidden-layers of a coordinate-MLP is implicitly related to the eigenvalue distribution of $\mathbf{X}^T\mathbf{X}$.

Remark 1 *Consider a set of coordinates $\{\mathbf{x}_i\}_{i=1}^N$ and the function $\phi(\cdot)$ induced by a hidden-layer of an MLP. Let $\{\lambda\}_{i=1}^N$ be the eigenvalues of $\mathbf{X}^T\mathbf{X}$ where $\mathbf{X} = [\phi(\mathbf{x}_1)^T \phi(\mathbf{x}_2)^T \dots \phi(\mathbf{x}_N)^T]$. Then, $\mathcal{S}(\mathbf{X}) = \sum_{i=1}^N \frac{\lambda_i}{\max_i(\lambda_i)}$ is a proxy measure for the Lipschitz smoothness of $\phi(\cdot)$. More precisely, if $\mathcal{S}(\mathbf{X})$ is larger, C tends to become larger, and vice-versa.*

the metric $\mathcal{S}(\cdot)$ is also known as the *stable rank* of a matrix. This is a useful result as computing the exact Lipschitz constant of an MLP is an NP-hard problem [35]. Although one can efficiently obtain upper-bounds for the Lipschitz constant, that requires calculating the gradients of the function. Instead, we can gain a rough understanding on the behavior of the Lipschitz smoothness of a particular layer by observing \mathcal{S} at run-time.

For optimal encoding performance, one should choose C to be in a *suitable* range that matches with the magnitude of the first-order gradients of the encoded signal. More precisely, these two factors maintain a monotonic relationship against each other. However, the derivatives (or the frequency) of a natural signal do not remain consistent across its domain. For instance, an image may contain high variations only within a subset of the pixels. Therefore, it is imperative that the hidden-layers of an MLP have the flexibility to model functions that have different Lipschitz smoothness across different intervals. In other words, we are interested in the *local* Lipschitz smoothness induced by the hidden-layers. In Section 3.4, we shall see that an MLP can gain this flexibility via suitably chosen activation functions.

In Section 3.4, we study the local Lipschitz smoothness of a hidden layer and connect it with the properties of activation functions.

3.4. Local Lipschitz smoothness

We are now interested in investigating the local Lipschitz smoothness of a hidden-layer. We formally define the local Lipschitz smoothness as follows:

Definition 1 A function $f : \mathbb{R}^m \rightarrow \mathbb{R}^n$ is locally Lipschitz around $\mathbf{x}_0 \in \mathbb{R}^m$ if for all $\mathbf{x} \in \mathbb{B}_\delta^m$ there exists a constant C such that $\|f(\mathbf{x}) - f(\mathbf{x}_0)\| \leq C\|\mathbf{x} - \mathbf{x}_0\|$ where \mathbf{x}_0 is the center \mathbf{x}_0 of \mathbb{B}_δ^m . Then, the smallest C for which the above inequality is satisfied is called the Lipschitz constant of f around \mathbf{x}_0 , and is denoted as $L_{\mathbf{x}_0, \delta}(f)$.

A hidden-layer is the composition of an affine function and a non-linearity. Hence, the composite local Lipschitz constant of a hidden-layer is upper-bounded with $L_{\mathbf{x}_0, \delta}(\psi \circ g) \leq L_{\mathbf{x}_0, \delta}(g)L_{\mathbf{x}_0, \delta}(\psi)$. Thus, we study these properties as δ approaches zero.

Affine transformations are differentiable, and hence, are locally Lipschitz by construction. Let $\mathbf{x} \in \mathbb{B}_\delta^m$ with center \mathbf{x}_0 . Then as $\lim_{\delta \rightarrow 0}$,

$$\|(\mathbf{A}\mathbf{x} + \mathbf{b}) - (\mathbf{A}\mathbf{x}_0 + \mathbf{b})\| \leq L_{\mathbf{x}_0, \delta}(g)\|\mathbf{x} - \mathbf{x}_0\| \quad (9)$$

$$L_{\mathbf{x}_0, \delta}(g) = \sup_{\|\mathbf{x} - \mathbf{x}_0\| \neq 0} \frac{\|\mathbf{A}(\mathbf{x} - \mathbf{x}_0)\|}{\|\mathbf{x} - \mathbf{x}_0\|}, \quad (10)$$

which is the operator norm of the weight matrix \mathbf{A} . We argue that manipulating the affine projections of an MLP is not an ideal as it can lead to drastic reduction of the search space of the fully connected layer, resulting in poor function approximations. Instead, we refrain from manipulating $L_{\mathbf{x}_0, \delta}(g)$ and focus on $L_{\mathbf{x}_0, \delta}(\psi)$.

Since ψ is a continuously differentiable function, applying the Taylor expansion gives

$$\psi(\mathbf{x}) = \psi(\mathbf{x}_0) + \mathbf{J}(\psi)_{\mathbf{x}_0}(\mathbf{x} - \mathbf{x}_0) + \Theta(\|\mathbf{x} - \mathbf{x}_0\|), \quad (11)$$

where $\Theta(\|\mathbf{x} - \mathbf{x}_0\|)$ is a rapidly decaying function as $\mathbf{x} \rightarrow \mathbf{x}_0$. Rearranging Eq. 11 we get

$$\|\psi(\mathbf{x}) - \psi(\mathbf{x}_0)\| \leq \|\mathbf{J}(\psi)_{\mathbf{x}_0}\|_o \|\mathbf{x} - \mathbf{x}_0\| + \Theta(\|\mathbf{x} - \mathbf{x}_0\|), \quad (12)$$

$$\lim_{\delta \rightarrow 0} \left[\sup_{\mathbf{x} \in \mathbb{B}_\delta^m} \frac{\|\psi(\mathbf{x}) - \psi(\mathbf{x}_0)\|}{\|\mathbf{x} - \mathbf{x}_0\|} \right] \leq \lim_{\delta \rightarrow 0} \left[\|\mathbf{J}(\psi)_{\mathbf{x}_0}\|_o + \frac{\Theta(\|\mathbf{x} - \mathbf{x}_0\|)}{\|\mathbf{x} - \mathbf{x}_0\|} \right]. \quad (13)$$

The left-hand side of Eq. 13 is the point-wise Lipschitz constant of $\psi(\cdot)$ at \mathbf{x}_0 by definition. Again, the quantity $\lim_{\delta \rightarrow 0} \frac{\Theta(\|\mathbf{x} - \mathbf{x}_0\|)}{\|\mathbf{x} - \mathbf{x}_0\|}$ is zero by definition. Thus, denoting the point-wise Lipschitz constant of $\psi(\cdot)$ at \mathbf{x}_0 as $L_{\mathbf{x}_0}(\psi)$, we get

$$L_{\mathbf{x}_0}(\psi) \leq \|\mathbf{J}(\psi)_{\mathbf{x}_0}\|_o. \quad (14)$$

Moreover, it can be shown that $\|\mathbf{J}(\psi)_{\mathbf{x}_0}\|_o \leq \|\mathbf{J}(\psi)_{\mathbf{x}_0}\|_F$ (Appendix) and hence,

$$L_{\mathbf{x}_0}(\psi) \leq \|\mathbf{J}(\psi)_{\mathbf{x}_0}\|_F. \quad (15)$$

Now, we present the following important remark that provides soft guidelines for selecting a proper activation function for coordinate-MLPs.

Remark 2 The activation function should ideally possess two important qualities: **Q1**) The local Lipschitz constant should have sufficient lower and upper bounds across the domain. Equivalently, the range of $\|\mathbf{J}(\psi)_x\|$ should appropriately match the magnitude of the first-order derivatives of the encoded signal. **Q2**) The local Lipschitz constant should smoothly vary across the domain of the activation function, so the composite function induced by the hidden-layers is allowed to project the points to appropriate subspaces, and achieve arbitrary local smoothness between the bounds. Equivalently, the second-order partial derivatives of $\psi(\cdot)$ should be non-zero and continuous over a considerable interval in the domain.

As established by Eq. 15, if a set of points are clustered very closely, the Lipschitz constant for those points can be obtained via the Jacobian norm of the activation function near the corresponding points. This gives us an important tool that can get an insight on the *maximum* local Lipschitz constant a network can achieve. For instance, let us choose a point-wise activation function. Then, $\mathbf{J}(f)_x$ is a diagonal matrix and we can bound L_x as follows:

$$L_x(\psi) \leq \sqrt{D(\max_{x \in \mathbb{R}} \psi'(x))^2}. \quad (16)$$

For $\mathbf{x} \in \mathbb{R}^D$ with a given layer width D . Since for a fixed network D is a constant,

$$\text{Range}(|\psi'(x)|) \quad (17)$$

provides us with a proxy metric to test **Q1**.

Intuitively, a layer of an MLP can achieve this upper bounds by projecting the points (via the affine transformation) to a small neighborhood where the highest first-order derivatives of the activation function exist. The test for **Q2** is simple: if the second derivative of the activation function is not negligible across a considerable interval (equivalently, if the local Lipschitz constant is smoothly varying across the domain of the activation), **Q2** is satisfied. Table 1 compares existing and several novel activation functions that we propose.

4. Experiments

In this section, we empirically validate the insights we gathered through our framework.

4.1. Comparison of activation functions

We compare the capacity of a coordinate-MLP in encoding signals when equipped with different activation functions. Fig. 2 illustrates an example where an image is encoded as the weights of an MLP. As shown, newly proposed Gaussian, Laplacian, ExpSin, and Quadratic activation functions are able to encode the image with significantly better fidelity with sharper gradients (high Lipschitz constants), compared to the existing activations such as ReLU, Tanh, SoftPlus, and SiLU. Also, note that the stable ranks (the energy distribution between the eigenvalues) of the hidden representations are higher for the proposed activation functions than the rest. This matches with our theoretical predictions by Remark 1.

4.2. Novel view synthesis

Without positional embeddings: We leverage the real synthetic dataset released by [22] to test the capacity of the Gaussian activations in encoding high-dimensional signals. Fig. 3 qualitatively contrasts the performance of ReLU vs. Gaussian activations without the positional embeddings. When the positional embeddings are not used, the ReLU MLPs demonstrate poor performance in capturing high-frequency details. On the contrary, Gaussian activations can capture information with higher fidelity in the absence of positional embedding. We believe this is an interesting result that opens up the possibility of positional-embedding-free architectures.

With positional embeddings: Although suitably chosen activation functions can omit positional embeddings, the combination of the two can still enable shallower networks

to learn high-frequency functions. Fig. 4 depicts an example with 4-layer MLPs. As evident, when the network is shallower, ReLU MLPs showcase reduced quality, while the performance of Gaussian activated MLPs is on-par with deeper ReLU MLPs. This advocates that practitioners can enjoy significantly cheaper architectures when properly designed activation functions are used. Table 2 depicts the quantitative results that include above comparisons.

4.3. Convergence

Sitzmann *et al.* comprehensively demonstrated that sine activations enable MLPs to encode signals with fine details. However, a drawback entailed with the sine activations is that they are extremely sensitive to the initialization of the MLP. In comparison, the proposed non-periodic activation functions do not suffer from such a problem. Fig. 5 illustrates a qualitative example. When the initialization method of the MLP does not strictly follow the method proposed in Sitzmann *et al.*, the sine activated MLPs do not converge even after 3000 epochs. In contrast, Gaussian activations demonstrate much faster convergence. Fig. 6 illustrates a quantitative comparison of convergence. We trained the networks on the natural image dataset released by [42] and the average PSNR value after each iteration is shown in Fig. 6. As clearly evident, the Gaussian activations enjoy higher robustness against the various initialization schemes of an MLP.

4.4. Local Lipschitz smoothness

As shown by Eq. 15, the local Lipschitz smoothness depends on the Jacobian norm of the corresponding point. In Section 3.4, we showed that a good proxy measure for the Lipschitz constant is the range of the first-order derivative of the activation function. We further affirmed that the Lipschitz constant should be suitably chosen for better performance *i.e.* a too high or too low Lipschitz constant can prevent the network from properly learning a signal. Fig. 7 illustrates an example that confirms this statement. When σ increases, $\text{Range}|\psi'|$ of the Gaussian activation decreases, decreasing the Lipschitz constant (see Eq. 17). In contrast, when a increases, the $\text{Range}|\psi'|$ of the sine activation increases, increasing the Lipschitz constant. A lower Lipschitz constant results in blurry edges as it does not allow sharp changes locally. On the other hand, an extremely large Lipschitz constant allows unwanted fluctuations. Hence, choosing the parameters to be in a suitable range is vital for better performance. Fig. 8 shows the distribution of local Lipschitz constants after encoding a signal with Gaussian activations with properly chosen parameters.

5. Conclusion

We seek to extend the current understanding of activation functions that allow coordinate-MLPs to encode functions

Activation (ψ)	Equation	parameterized	ψ'	ψ''	Q1	Q2
ReLU	$\max(0, x)$	\times	$\begin{cases} 1, & \text{if } x > 0 \\ 0, & \text{otherwise} \end{cases}$	0	\times	\times
PReLU	$\begin{cases} x, & \text{if } x > 0 \\ ax, & \text{otherwise} \end{cases}$	\checkmark	$\begin{cases} 1, & \text{if } x > 0 \\ a, & \text{otherwise} \end{cases}$	0	\checkmark	\times
Sin	$\sin(ax)$	\checkmark	$\cos(ax)$	$-a^2 \sin(ax)$	\checkmark	\checkmark
Tanh	$\frac{e^x - e^{-x}}{e^x + e^{-x}}$	\times	$\frac{4e^{2x}}{(e^{2x} + 1)^2}$	$-\frac{8(e^{2x} - 1)e^{2x}}{(e^{2x} + 1)^3}$	\times	\checkmark
Sigmoid	$\frac{1}{1 + e^{-x}}$	\times	$\frac{e^x}{(e^x + 1)^2}$	$-\frac{(e^x - 1)e^x}{(e^x + 1)^3}$	\times	\checkmark
SiLU	$\frac{x}{1 + e^{-x}}$	\times	$\frac{e^x(e^x + 1)^2}{(e^x + 1)^2}$	$-\frac{e^x((x-2)e^x - x - 2)}{(e^x + 1)^3}$	\times	\checkmark
SoftPlus	$\frac{1}{a} \log(1 + e^{ax})$	\checkmark	$\frac{e^{cx}}{1 + e^{cx}}$	$-\frac{ce^{cx}}{(e^{cx} + 1)^2}$	\checkmark	\times
Gaussian	$e^{-\frac{0.5x^2}{a^2}}$	\checkmark	$-\frac{x}{a^2}$	$(x^2 - a^2)e^{-\frac{x^2}{2a^2}}$	\checkmark	\checkmark
Quadratic	$\frac{1}{1 + (ax)^2}$	\checkmark	$-\frac{2ax}{(a^2x^2 + 1)^2}$	$\frac{2a^2(3a^2x^2 - 1)}{(a^2x^2 + 1)^3}$	\checkmark	\checkmark
Multi Quadratic	$\frac{1}{\sqrt{1 + (ax)^2}}$	\checkmark	$-\frac{a^2x}{(a^2x^2 + 1)^{\frac{3}{2}}}$	$\frac{2a^4x^2 - a^2}{(a^2x^2 + 1)^{\frac{5}{2}}}$	\checkmark	\checkmark
Laplacian	$e(-\frac{ x }{a})$	\checkmark	$\frac{ x }{a}$	$\frac{ x }{a^2}$	\checkmark	\checkmark
Super-Gaussian	$[e^{-\frac{0.5x^2}{a^2}}]^b$	\checkmark	$-\frac{bx}{a^2}$	$b(bx^2 - a^2)e^{-\frac{bx^2}{2a^2}}$	\checkmark	\checkmark
ExpSin	$e^{\sin(ax)}$	\checkmark	$ae^{\sin(ax)} \cos(ax)$	$-a^2 e^{\sin(ax)} (\sin(ax) - \cos^2(ax))$	\checkmark	\checkmark

Table 1. **Comparison of existing activation functions (top block) against the proposed activation functions (bottom block).** The proposed activations and the sine activations fulfill **Q1** and **Q2** in Remark 2, implying better suitability to encode high-frequency signals.

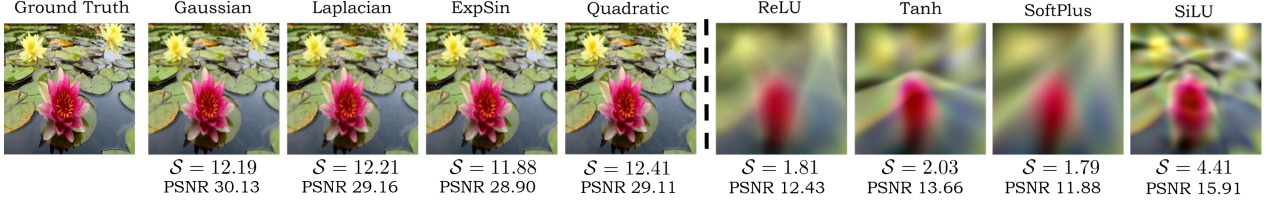


Figure 2. **Proposed activations (left block) vs. existing activations (right block) and their respective stable ranks (S) in image encoding without positional embeddings.** As predicted by Remark 2, the proposed activations are better suited for encoding signals with high fidelity. As Remark 1 stated, the stable ranks of the proposed activations are higher, indicating larger local Lipschitz constants which allow sharper gradients.



Figure 3. **Novel view synthesis without positional embedding (zoom in for a better view).** Gaussian activations can completely omit positional embeddings while producing results with significantly better fidelity. In contrast, the performance of ReLU-MLPs severely degrade when positional embeddings are not used. We use 8-Layer MLPs for this experiment.

with high fidelity. We show that the previously proposed sinusoid activation [40] is a single example of a much broader

class of activation functions that enable coordinate-MLPs to encode high-frequency signals. Further, we develop generic



Figure 4. **Novel view synthesis with positional embedding (zoom in for a better view).** With Gaussian activations, shallow MLPs can obtain high-fidelity reconstructions. In contrast, the performance of ReLU-MLPs degrade when the depth of the MLP reduces. We use 4-layer MLPs for this comparison.

Activation	Depth	PE	PSNR	SSIM
ReLU	4L	✓	27.44	0.922
Gaussian	4L	✓	31.13	0.947
ReLU	8L	✗	26.55	0.918
Gaussian	8L	✗	31.17	0.949
ReLU	8L	✓	30.91	0.941
Gaussian	8L	✓	31.58	0.951

Table 2. **Quantitative comparison in novel view synthesis on the real synthetic dataset [22].** Gaussian activations can achieve high-fidelity reconstructions without positional embeddings. When equipped with positional embeddings, they demonstrate similar performance with $\sim 50\%$ less parameters.



Figure 5. **Qualitative comparison of convergence when MLPs are initialized without following [39] (after 3000 epochs).** Unlike sine activations, Gaussian activations are robust to various initialization schemes (example shown used Xavier normal initialization).

guidelines to devise and tune an activation function for coordinate-MLPs and propose several non-periodic activation functions as examples. Finally, choosing Gaussian ac-

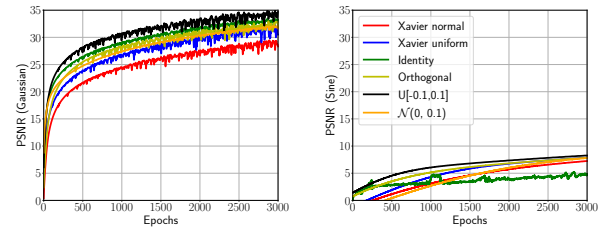


Figure 6. **Convergence rates of Gaussian and sine MLPs on natural images by [42] under different initialization schemes.** Gaussian activations are significantly robust to various initialization methods compared to sine activations. Other proposed non-periodic activation functions (not shown in the figure) also demonstrate similar robustness. However, sine activations show a similar convergence rate to Gaussians when the MLPs are initialized strictly following the guidelines of [39].

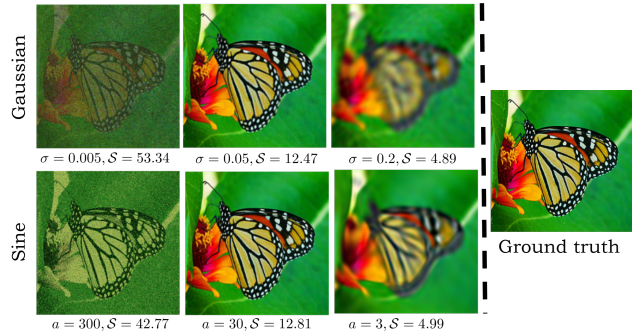


Figure 7. **Stable rank (S) vs the fidelity of reconstructions.** Having an extremely high or low stable rank (or equivalently a Lipschitz constant) hampers the ability of an MLP in encoding functions with fine details (Remark 1). Thus, it is important to adjust the hyper-parameters of an activation function to tune the above metrics to a suitable range.

tivations from the proposed list, we demonstrate compelling results across various signal encoding tasks.



Figure 8. **Distribution of the upperbound of the point-wise Lipschitz constant $\|\mathbf{J}(f)_x\|_F$ (Eq. 15) with Gaussian reconstructions.** Having an activation function with a suitable bound for the local Lipschitz constant helps the network to learn functions with properly distributed derivatives.

References

- [1] Abol Basher, Muhammad Sarmad, and Jani Boutellier. Lightsal: Lightweight sign agnostic learning for implicit surface representation. *arXiv preprint arXiv:2103.14273*, 2021. 1, 3
- [2] Ronen Basri, Meirav Galun, Amnon Geifman, David Jacobs, Yoni Kasten, and Shira Kritchman. Frequency bias in neural networks for input of non-uniform density. In *International Conference on Machine Learning*, pages 685–694. PMLR, 2020. 2
- [3] Eric B Baum and Frank Wilczek. Supervised learning of probability distributions by neural networks. In *Neural information processing systems*, volume 12, pages 52–61. New York, NY, 1988. 2
- [4] Jinde Cao and Jun Wang. Absolute exponential stability of recurrent neural networks with lipschitz-continuous activation functions and time delays. *Neural networks*, 17(3):379–390, 2004. 2
- [5] Zhiqin Chen and Hao Zhang. Learning implicit fields for generative shape modeling. In *Proceedings of the IEEE/CVF Conference on Computer Vision and Pattern Recognition*, pages 5939–5948, 2019. 1, 3
- [6] Bhaskar DasGupta and Georg Schnitger. The power of approximation: A comparison of activation functions. In *NIPS*, pages 615–622. Denver, CO, 1992. 2
- [7] Boyang Deng, John P Lewis, Timothy Jeruzalski, Gerard Pons-Moll, Geoffrey Hinton, Mohammad Norouzi, and Andrea Tagliasacchi. Nasa neural articulated shape approximation. In *Computer Vision–ECCV 2020: 16th European Conference, Glasgow, UK, August 23–28, 2020, Proceedings, Part VII 16*, pages 612–628. Springer, 2020. 1, 3
- [8] Jerome A. Feldman, Mark A. Fenty, and Nigel H Goodard. Computing with structured neural networks. *Computer*, 21(3):91–103, 1988. 2
- [9] A Ronald Gallant and Halbert White. There exists a neural network that does not make avoidable mistakes. In *ICNN*, pages 657–664, 1988. 2
- [10] Kyle Genova, Forrester Cole, Avneesh Sud, Aaron Sarna, and Thomas Funkhouser. Local deep implicit functions for 3d shape. In *Proceedings of the IEEE/CVF Conference on Computer Vision and Pattern Recognition*, pages 4857–4866, 2020. 1, 3
- [11] Philipp Henzler, Niloy J Mitra, and Tobias Ritschel. Learning a neural 3d texture space from 2d exemplars. In *Proceedings of the IEEE/CVF Conference on Computer Vision and Pattern Recognition*, pages 8356–8364, 2020. 1
- [12] John J Hopfield. Neurons with graded response have collective computational properties like those of two-state neurons. *Proceedings of the national academy of sciences*, 81(10):3088–3092, 1984. 2
- [13] John J Hopfield and David W Tank. Computing with neural circuits: A model. *Science*, 233(4764):625–633, 1986. 2
- [14] Bekir Karlik and A Vehbi Olgac. Performance analysis of various activation functions in generalized mlp architectures of neural networks. *International Journal of Artificial Intelligence and Expert Systems*, 1(4):111–122, 2011. 2
- [15] Renée Koplon and Eduardo D Sontag. Using fourier-neural recurrent networks to fit sequential input/output data. *Neurocomputing*, 15(3-4):225–248, 1997. 2
- [16] Xue-Bin Liang and Jun Wang. Absolute exponential stability of neural networks with a general class of activation functions. *IEEE Transactions on Circuits and Systems I: Fundamental Theory and Applications*, 47(8):1258–1263, 2000. 2
- [17] Xue-Bin Liang and Jun Wang. An additive diagonal-stability condition for absolute exponential stability of a general class of neural networks. *IEEE Transactions on circuits and systems I: Fundamental Theory and Applications*, 48(11):1308–1317, 2001. 2
- [18] Peng Liu, Zhigang Zeng, and Jun Wang. Multistability of recurrent neural networks with nonmonotonic activation functions and mixed time delays. *IEEE Transactions on Systems, Man, and Cybernetics: Systems*, 46(4):512–523, 2015. 2
- [19] Wenlian Lu and Tianping Chen. Dynamical behaviors of cohen–grossberg neural networks with discontinuous activation functions. *Neural Networks*, 18(3):231–242, 2005. 2
- [20] Liying Ma and Khashayar Khorasani. Constructive feed-forward neural networks using hermite polynomial activation functions. *IEEE Transactions on Neural Networks*, 16(4):821–833, 2005. 2
- [21] Ricardo Martin-Brualla, Noha Radwan, Mehdi SM Sajjadi, Jonathan T Barron, Alexey Dosovitskiy, and Daniel Duckworth. Nerf in the wild: Neural radiance fields for unconstrained photo collections. In *Proceedings of the IEEE/CVF Conference on Computer Vision and Pattern Recognition*, pages 7210–7219, 2021. 1, 3
- [22] Ben Mildenhall, Pratul P Srinivasan, Matthew Tancik, Jonathan T Barron, Ravi Ramamoorthi, and Ren Ng. Nerf: Representing scenes as neural radiance fields for view synthesis. In *European Conference on Computer Vision*, pages 405–421. Springer, 2020. 1, 2, 3, 6, 8

- [23] Jiteng Mu, Weichao Qiu, Adam Kortylewski, Alan Yuille, Nuno Vasconcelos, and Xiaolong Wang. A-sdf: Learning disentangled signed distance functions for articulated shape representation. *arXiv preprint arXiv:2104.07645*, 2021. 1, 3
- [24] Alan Murray, Anthony Smith, and Zoe Butler. Bit-serial neural networks. In *Neural Information Processing Systems*, pages 573–583, 1987. 2
- [25] Michael Niemeyer, Lars Mescheder, Michael Oechsle, and Andreas Geiger. Differentiable volumetric rendering: Learning implicit 3d representations without 3d supervision. In *Proceedings of the IEEE/CVF Conference on Computer Vision and Pattern Recognition*, pages 3504–3515, 2020. 1, 3
- [26] Michael Oechsle, Lars Mescheder, Michael Niemeyer, Thilo Strauss, and Andreas Geiger. Texture fields: Learning texture representations in function space. In *Proceedings of the IEEE/CVF International Conference on Computer Vision*, pages 4531–4540, 2019. 1
- [27] Jeong Joon Park, Peter Florence, Julian Straub, Richard Newcombe, and Steven Lovegrove. Deepsdf: Learning continuous signed distance functions for shape representation. In *Proceedings of the IEEE/CVF Conference on Computer Vision and Pattern Recognition*, pages 165–174, 2019. 1, 3
- [28] Keunhong Park, Utkarsh Sinha, Jonathan T Barron, Sofien Bouaziz, Dan B Goldman, Steven M Seitz, and Ricardo Martin-Brualla. Nerfies: Deformable neural radiance fields. In *Proceedings of the IEEE/CVF International Conference on Computer Vision*, pages 5865–5874, 2021. 1, 3
- [29] Dabal Pedamonti. Comparison of non-linear activation functions for deep neural networks on mnist classification task. *arXiv preprint arXiv:1804.02763*, 2018. 2
- [30] Albert Pumarola, Enric Corona, Gerard Pons-Moll, and Francesc Moreno-Noguer. D-nerf: Neural radiance fields for dynamic scenes. In *Proceedings of the IEEE/CVF Conference on Computer Vision and Pattern Recognition*, pages 10318–10327, 2021. 1, 3
- [31] Nasim Rahaman, Aristide Baratin, Devansh Arpit, Felix Draxler, Min Lin, Fred Hamprecht, Yoshua Bengio, and Aaron Courville. On the spectral bias of neural networks. In *International Conference on Machine Learning*, pages 5301–5310. PMLR, 2019. 2
- [32] Prajit Ramachandran, Barret Zoph, and Quoc V Le. Searching for activation functions. *arXiv preprint arXiv:1710.05941*, 2017. 2
- [33] Daniel Rebain, Wei Jiang, Soroosh Yazdani, Ke Li, Kwang Moo Yi, and Andrea Tagliasacchi. Derf: Decomposed radiance fields. In *Proceedings of the IEEE/CVF Conference on Computer Vision and Pattern Recognition*, pages 14153–14161, 2021. 1, 3
- [34] Shunsuke Saito, Zeng Huang, Ryota Natsume, Shigeo Morishima, Angjoo Kanazawa, and Hao Li. Pifu: Pixel-aligned implicit function for high-resolution clothed human digitization. In *Proceedings of the IEEE/CVF International Conference on Computer Vision*, pages 2304–2314, 2019. 1, 3
- [35] Kevin Scaman and Aladin Virmaux. Lipschitz regularity of deep neural networks: analysis and efficient estimation. *arXiv preprint arXiv:1805.10965*, 2018. 4
- [36] Sagar Sharma, Simone Sharma, and Anidhya Athaiya. Activation functions in neural networks. *towards data science*, 6(12):310–316, 2017. 2
- [37] P Sibi, S Allwyn Jones, and P Siddarth. Analysis of different activation functions using back propagation neural networks. *Journal of theoretical and applied information technology*, 47(3):1264–1268, 2013. 2
- [38] Adrian Silvescu. Fourier neural networks. In *IJCNN’99. International Joint Conference on Neural Networks. Proceedings (Cat. No. 99CH36339)*, volume 1, pages 488–491. IEEE, 1999. 2
- [39] Vincent Sitzmann, Julien Martel, Alexander Bergman, David Lindell, and Gordon Wetzstein. Implicit neural representations with periodic activation functions. *Advances in Neural Information Processing Systems*, 33, 2020. 1, 2, 3, 8
- [40] Vincent Sitzmann, Michael Zollhöfer, and Gordon Wetzstein. Scene representation networks: Continuous 3d-structure-aware neural scene representations. *arXiv preprint arXiv:1906.01618*, 2019. 1, 3, 7
- [41] Josep M Sopena, Enrique Romero, and Rene Alquezar. Neural networks with periodic and monotonic activation functions: a comparative study in classification problems. 1999. 2
- [42] Matthew Tancik, Pratul P Srinivasan, Ben Mildenhall, Sara Fridovich-Keil, Nithin Raghavan, Utkarsh Singhal, Ravi Ramamoorthi, Jonathan T Barron, and Ren Ng. Fourier features let networks learn high frequency functions in low dimensional domains. *arXiv preprint arXiv:2006.10739*, 2020. 2, 6, 8, 13, 14
- [43] Garvita Tiwari, Nikolaos Sarafianos, Tony Tung, and Gerard Pons-Moll. Neural-gif: Neural generalized implicit functions for animating people in clothing. In *Proceedings of the IEEE/CVF International Conference on Computer Vision*, pages 11708–11718, 2021. 1, 3
- [44] Zirui Wang, Shangzhe Wu, Weidi Xie, Min Chen, and Victor Adrian Prisacariu. Nerf-: Neural radiance fields without known camera parameters. *arXiv preprint arXiv:2102.07064*, 2021. 1, 3
- [45] Ronald J Williams. The logic of activation functions. *Parallel distributed processing: Explorations in the microstructure of cognition*, 1:423–443, 1986. 2
- [46] Kwok-wo Wong, Chi-sing Leung, and Sheng-jiang Chang. Handwritten digit recognition using multilayer feedforward neural networks with periodic and monotonic activation functions. In *Object recognition supported by user interaction for service robots*, volume 3, pages 106–109. IEEE, 2002. 2
- [47] Fanbo Xiang, Zexiang Xu, Milos Hasan, Yannick Hold-Geoffroy, Kalyan Sunkavalli, and Hao Su. Neutex: Neural texture mapping for volumetric neural rendering. In *Proceedings of the IEEE/CVF Conference on Computer Vision and Pattern Recognition*, pages 7119–7128, 2021. 1
- [48] Alex Yu, Vickie Ye, Matthew Tancik, and Angjoo Kanazawa. pixelnerf: Neural radiance fields from one or few images. In *Proceedings of the IEEE/CVF Conference on Computer Vision and Pattern Recognition*, pages 4578–4587, 2021. 1, 3

- [49] Jianqiao Zheng, Sameera Ramasinghe, and Simon Lucey. Rethinking positional encoding. *arXiv preprint arXiv:2107.02561*, 2021. [2](#)

Appendix

A. Proof for Proposition 1

By continuity, for each $x \in \mathbb{R}$, there exists $\alpha(x) > 0$ such that $|f(\bar{x}) - f(x)| < \epsilon/2$ for all \bar{x} with $|\bar{x} - x| < \alpha(x)$. Consider the open intervals $(x - \alpha(x)/2, (x + \alpha(x)/2)$ with $t \leq x \leq t + 1$ covering the compact intervals $[t, t + 1]$. Let $t = x_0 < x_1 < \dots < x_n = t + 1$ be centers of finitely many subintervals. Let $g(x) = \frac{g(x_{i+1}) - g(x_i)}{(x_{i+1} - x)}(x - x_i) + g(x_i)$, $\forall x_i < x < x_{i+1}$ be a function through all x_i . Then, $|g(x) - f(x)| < \epsilon$ because for $0 < i < n$, we have $|x_i - x_{i+1}| < \max\{\alpha(x_i), \alpha(x_{i+1})\}$. Then, for $x \in [x_i, x_{i+1}]$, either $|g(x) - f(x)| \leq |g(x) - g(x_i)| + |f(x) - f(x_i)| < \epsilon$ or $|g(x) - f(x)| \leq |g(x) - g(x_{i+1})| + |f(x) - f(x_{i+1})| < \epsilon$. Therefore, $g(x)$ converges to $f(x)$ uniformly.

Now, consider a small interval κ such that for $x \in \kappa$, $g(x) \approx f(x)$. For a seen pair of points $x_k, x_{k+1} \in \kappa$, we have $g(x_k) = \mathbf{A}\phi(x_k)$ and $g(x_{k+1}) = \mathbf{A}\phi(x_{k+1})$. In order to regress a point x such that $x_k < x < x_{k+1}$, we need,

$$\frac{\mathbf{A}(\phi(x_{k+1}) - \phi(x_k))}{x_{k+1} - x_k} = \frac{\mathbf{A}(\phi(x) - \phi(x_k))}{x - x_k} \quad (18)$$

Assume $\frac{x_{k+1} - x_k}{x - x_k} = T$ is a rational number. Then,

$$\sup \left[\frac{\|\mathbf{A}(\phi(x_{k+1}) - \phi(x_k))\|}{T\|(\phi(x) - \phi(x_k))\|} \right] = \|\mathbf{A}\|_o \quad (19)$$

In order for the left side to become the operator norm,

$$T\|(\phi(x) - \phi(x_k))\| = \|(\phi(x_{k+1}) - \phi(x_k))\| \quad (20)$$

$$\frac{\|(\phi(x) - \phi(x_k))\|}{x - x_k} = \frac{\|(\phi(x_{k+1}) - \phi(x_k))\|}{x_{k+1} - x_k} = K \quad (21)$$

□

B. Encoding signals

Embedding	Image type	PSNR
ReLU	Natural	20.42
Tanh	Natural	16.91
SoftPlus	Natural	16.03
SiLU	Natural	17.59
Gaussian	Natural	33.43
Laplacian	Natural	33.01
Quadratic	Natural	32.90
Multi-Quadratic (e. tr.)	Natural	33.11
ExpSin	Natural	32.99
Super-Gaussian	Natural	33.12
ReLU	Text	18.49
Tanh	Text	16.19
SoftPlus	Text	15.77
SiLU	Text	17.43
Gaussian	Text	36.17
Laplacian	Text	36.29
Quadratic	Text	35.55
Multi-Quadratic	Text	36.20
ExpSin	Text	35.89
Super-Gaussian	Text	35.57
ReLU	Noise	10.82
Tanh	Noise	9.66
SoftPlus	Noise	9.71
SiLU	Noise	11.21
Gaussian	Noise	11.78
Laplacian	Noise	11.01
Quadratic	Noise	11.67
Multi-Quadratic	Noise	11.29
ExpSin	Noise	11.45
Super-Gaussian	Noise	11.33

Table 3. **Quantitative comparison between activations in 2D signal encoding on [42] after 3000 epochs.** The proposed activations yield high PSNRs.



Figure 9. Qualitative examples of 2D signal encoding using the proposed activations on the natural images by [42].

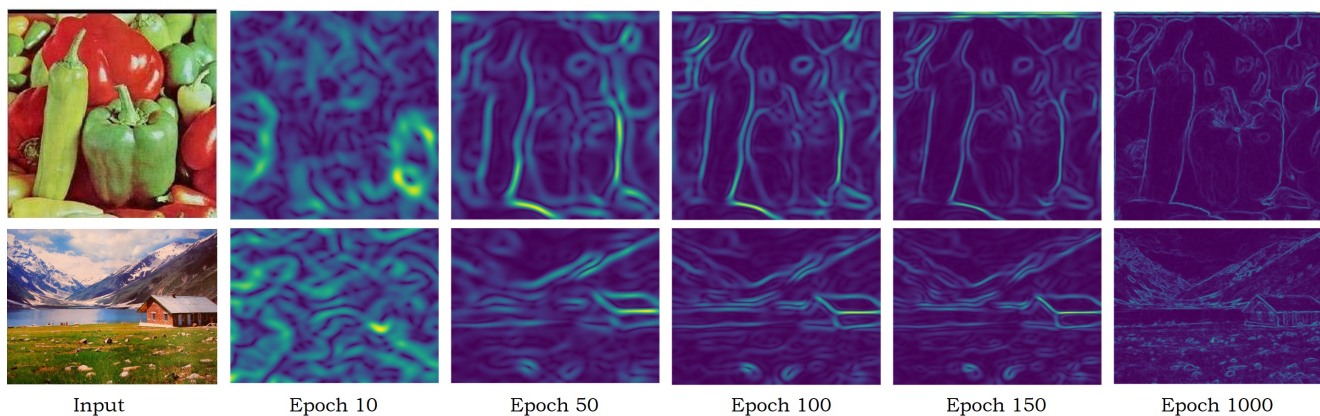


Figure 10. $\|\mathbf{J}_f(\mathbf{x})\|_F$ convergence as the training progresses.

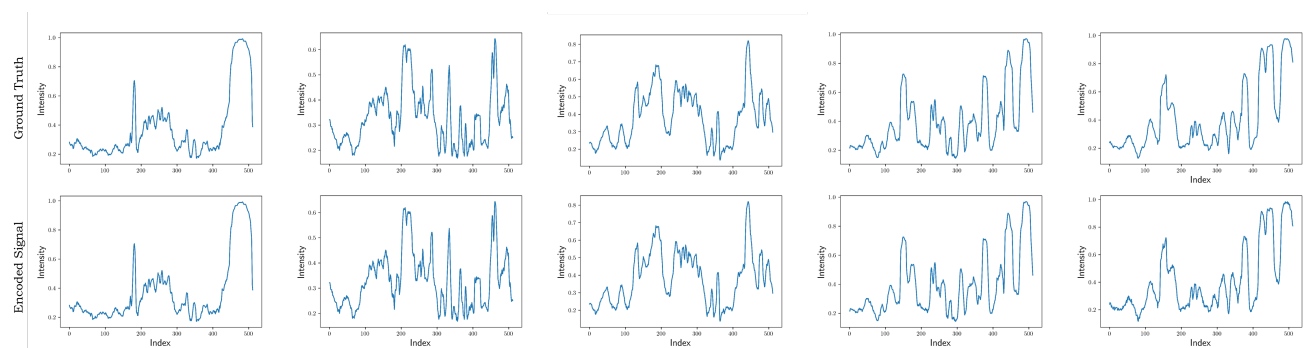


Figure 11. 1D signal encoding using Gaussian activated MLPs.